PAPER • OPEN ACCESS

Investigation of mechanical responses of underground fortifications at different explosion distances

To cite this article: Qindong Lin *et al* 2023 *J. Phys.: Conf. Ser.* **2660** 012009

View the article online for updates and enhancements.

Investigation of mechanical responses of underground fortifications at different explosion distances

Qindong Lin[1], Chun Feng[2], Yulei Zhang[1*], Yundan Gan[1], Jianfei Yuan[1] and Wenjun Jiao[1]

[1]Xi'an Modern Chemistry Research Institute, Xi'an, Shaanxi, 710065, China

[2]Institute of Mechanics, Chinese Academy of Sciences, Beijing 100190, China

Corresponding author: 413190021@qq.com

Abstract: The mechanical responses of underground fortifications subjected to blast loading is an important topic related to survival and security ability. Based on a FEM-DEM coupled algorithm, the difference in mechanical responses of underground fortifications subjected to different blast loadings is studied. Firstly, full-time numerical simulations of underground fortifications are conducted. Then, the mechanical characteristics (i.e., displacement and crack) of underground fortifications are analyzed quantitatively. The result indicates that the maximum displacement of underground fortifications gradually reduces from 3.35 m to 1.90 m when the horizontal distance D_H increases, and the rock volume V_C and V_F gradually decrease with the increase of D_H. The crack ratio at the same moment gradually decreases with the increase of D_H, and the spatial distribution of fracture type changes significantly with the increase of D_H.

1. Introduction

The mechanical responses characteristic of engineering structures (e.g., underground civil defense project, protective engineering and tunnel) under the explosion shock wave is a key issue related to the survival and security ability of underground fortifications under the conditions of war or accidental explosion. Therefore, there is a need to investigate the mechanical response process of underground fortifications under the explosion shock wave [1-3].

In recent years, many scholars conduct extensive research on the mechanical responses of underground fortifications subjected to blast loading using experimental study, theoretical analysis and numerical simulation. Jiang and Zhou [4] proposed that the maximum vertical vibration velocity is the main role in blasting vibration control. Ma [5] researched the blast vibration effects of underground pipelines under explosion loading, and the results indicated that the shock wave causes three types of failure behavior in concrete pipelines. Fan et al. [6] simplified the elastic resistances as elastic chain-pole and obtained the moment and displacement of the underground structure.

Due to the expensive cost of experimental study and the limitation of theoretical analysis, Zhao et al. [7] established an "explosive-air-structure-soil" numerical model, and the results indicated that the shock wave converges at the far-end for a long time, which is the weak part of a tunnel. Using the LS-DYNA software, Ma et al. [8] proposed that the maximum displacement increases with the growth of structure span, and decreases with the growth of structure thickness. Kong et al. [9] simulated the mechanical responses of underground arch structures for different rock types and different spans under vertical blast loading, and proposed that the harder the rock is, the stronger the vault dynamic interaction is. Rashiddel et al. [10] studied the tunnel planar and curved joint segments subjected to dynamic loads

and proposed that the curved joint segmented lining is effective and stable. Zhu et al. [11] studied the mechanical responses of ground motions and surrounding fortifications subjected to the blast-induced shock wave.

Many scholars carried out the numerical simulation on the mechanical responses of underground fortifications subjected to blast loading, while the numerical methods mainly belong to continuum mechanics methods, (e.g., finite difference method (FDM), finite volume method (FVM), finite element method (FEM)). Since the algorithms mainly simulate the expansion of crack by deleting elements, which cannot accurately characterize the crack characteristics of the numerical model. Based on a FEM-DEM coupled method, this paper studies the influences of explosion distances on the dynamic mechanical responses of underground fortifications, which lays the foundation for the subsequent analysis of the striking effect of earth penetrators on underground fortifications.

2. Simulation

2.1. Model

In the research, the continuum-discontinuum element method (CDEM) is introduced, which achieves a conversion of mass and energy. Figure 1 plots the numerical model, which includes rock mass, explosives and underground fortifications, and it is composed of concrete. The horizontal dimension of rock masses is L_{rh} = 150 m, and the vertical dimension of rock masses is L_{rv} = 100 m. The horizontal dimension of underground fortifications is L_{fh} = 15 m, the vertical dimension of underground fortifications is L_{fv} = 10 m, and the concrete wall thickness of underground fortifications is L_{ft} = 1.8 m. The diameter of explosives is 0.2 m, and they are 10 m away from the underground fortifications in the vertical direction. For the four cases, the horizontal distance between the midpoint of fortifications and the explosives changes from 0 m to 15 m. The triangular element is introduced to mesh the numerical model, and three mesh sizes are set for the mesh division. The element size of explosive L_e = 0.05 m, the element size of concrete L_c = 0.20 m, and the element size of rock masses L_r = 1.00 m. Table 1 lists the mechanical parameters of rock mass and concrete.
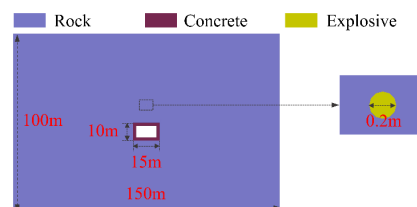

Figure 1. 2D Numerical models of rock mass and underground fortifications

Table 1. Basic parameters of concrete and rock mass

Type	Density (kg/m^3)	Tensile strength (GPa)	Young's modulus (GPa)	Cohesive strength (GPa)
Rock mass	2.3e3	3e-3	1e1	7e-3
Concrete	2.5e3	9e-3	3.5e1	1.8e-2

2.2. Simulation results

The horizontal distance D_H from the midpoint of underground fortifications to the explosive is set to four values, D_H = 0 m for case I, D_H = 5 m for case II, D_H = 10 m for case III and D_H = 15 m for case IV.

2.2.1. Displacement characteristic

Due to the difference in horizontal distance D_H in the four cases, the rendezvous position between the wavefront and the underground fortifications during the outward propagation process of shock wave changes, which leads to the difference in spatial movement of underground fortifications. Figure 2 plots the displacement nephograms of underground fortifications in the four cases when the time t = 0.1 s. It

can be concluded that the maximum value of displacement of underground fortifications gradually reduces from 3.35 m to 1.90 m with the increase of the horizontal distance D_H from 0 m to 15 m. This is because when the horizontal distance D_H increases, the intensity of the shock wave arriving at the underground fortifications gradually weakens.

In the case of $D_H = 0$ m, the blast loading applied at the concrete of the top boundary is strong, which induces a larger displacement of the concrete, and the displacement at the middle part is the same, which is the maximum value of the whole model. The concrete at the bottom, right and left boundaries also undergoes crack and slippage, but the displacement is small.

In the case of $D_H = 5$ m, the concrete at the left and left boundaries undergoes a large displacement. For the concrete of the top boundary, the displacement increases and then reduces when the distance from the left endpoint increases, and the maximum displacement is located between the left endpoint and the midpoint. For the left boundary, as the increase of distance from the top endpoint, the displacement of concrete increases and then reduces, and the displacements of concrete at the midpoint of the left boundary are maximum. During the movement of concrete, the concrete at the top boundary arrives at the left boundary, which causes changes in the movement characteristics of the concrete. The concrete at the bottom boundary and right boundary also undergoes fracture and slippage, but the displacement is small.

In the case of $D_H = 10$ m, the concrete at the left and top boundaries undergoes large displacement, and the concrete at the bottom boundary and right boundary also undergoes fracture. For the top boundary, as the distance from the left endpoint increases, the change trend of displacement first is different, and the maximum value is located between the left endpoint and the midpoint. For the concrete of left boundaries, the growth trend of displacement first also changes when the distance from the top endpoint increases, and the maximum displacement occurs between the top endpoint and the midpoint. It is observed that the spatial distribution of displacement in the case of $D_H = 5$ m and $D_H = 10$m are similar, but the value is different.

In the case of $D_H = 15$ m, the concrete at the top and left boundaries undergoes large displacement, and the concrete at the right and bottom boundaries also undergoes crack and slippage, but the displacement value is small. For the top boundary, as the distance from the left endpoint increases, the growth trend of displacement also changes, and the maximum value is located approximately at the midpoint. For the left boundaries, the growth trend of displacement changes when the distance from the top endpoint increases, the maximum displacement is located between the bottom endpoint and the midpoint, and the concrete at the left and top boundaries has not yet collided.

(a) $D_H = 0$ m   (b) $D_H = 5$ m
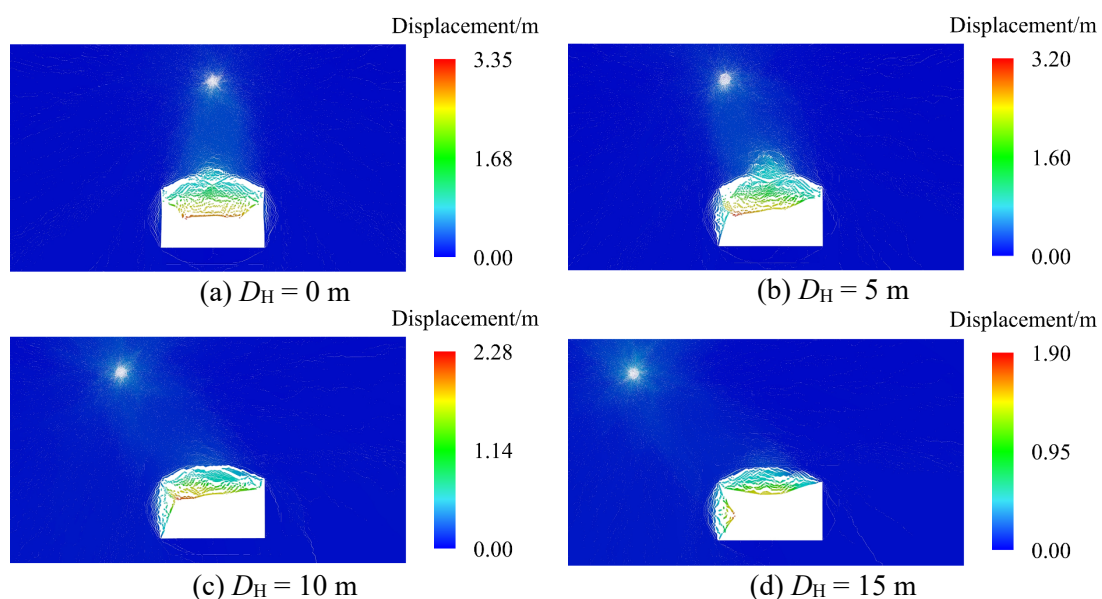
(c) $D_H = 10$ m   (d) $D_H = 15$ m

Figure 2. Spatial movement nephograms of underground fortifications at $t = 0.1$ s

Since the concrete wall of underground fortifications loses its load-bearing capacity, the rock above collapses and enters into the underground fortifications. Figure 3 plots the volume V_F of rock mass that enters into the underground fortifications and the volume V_C of collapsed rock at $t = 1.0$ s. It is seen that the change trends of V_C and V_F are similar, and V_C is always larger than V_F, which indicates that there is a large amount of rock that collapses but not enters into the underground fortifications. With the increase of D_H, V_C and V_F gradually decrease, and V_C and V_F decrease to 0 when $D_H = 15$m. The decreasing ratio of V_C and V_F is not a constant value, as the horizontal distance D_H increases, the decreasing ratio of V_C and V_F increases firstly and decreases.
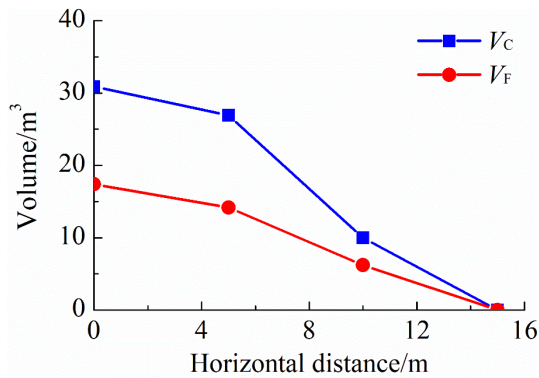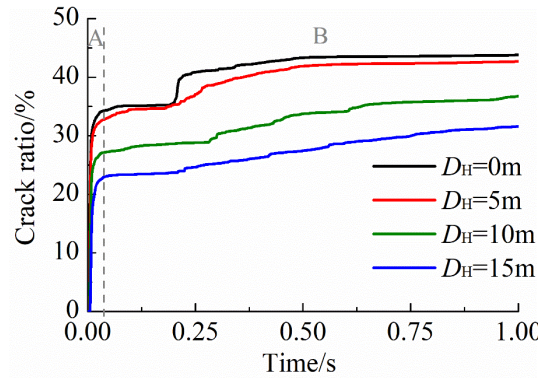

Figure 3. Curve of V_C and V_F when $t = 1.0$ s

Figure 4. Change trend of crack ratio α

2.2.2. Crack

Figure 4 plots the change trend of crack ratio α in different cases. It is observed that the change trend of the crack ratio is similar in different cases, and the crack ratio α at the same moment gradually decreases with the increase of D_H. During stage A, the crack ratio α increases sharply with the growth of time. This is due to the fact that the intensity of the shock wave arriving at the underground fortifications for the first time is very strong, which causes a large number of interfaces to crack. In stage B, since the intensity of the shock wave decays sharply, the destructive effect on the underground fortifications is weakened, and the crack ratio α increases slowly with the growth of time.

Figure 5 plots the initial fracture nephograms of underground fortifications and rock mass, and it is seen that the initial fracture nephograms of underground fortifications change significantly with the increase of D_H. For the concrete interface at the top boundary, most of them at the middle part undergo tensile fracture in the case of $D_H = 0$ m, and most of them at the left part undergo tensile fracture in the case of $D_H = 5$ m. With the increase of D_H, the number of concrete interfaces that undergo tensile fracture gradually decreases. For the left and right boundaries, the number of cracked interfaces at the left boundary gradually increases as the increase of D_H, while the number of cracked interfaces at the right boundaries gradually decreases. For the bottom boundary, with the increase of D_H, most of the interfaces undergo tensile fracture, but the number of cracked interfaces gradually decreases. It is concluded that with the increase of horizontal distance D_H, not only the number of cracked interface changes, but also the spatial distribution characteristic of fracture type changes.
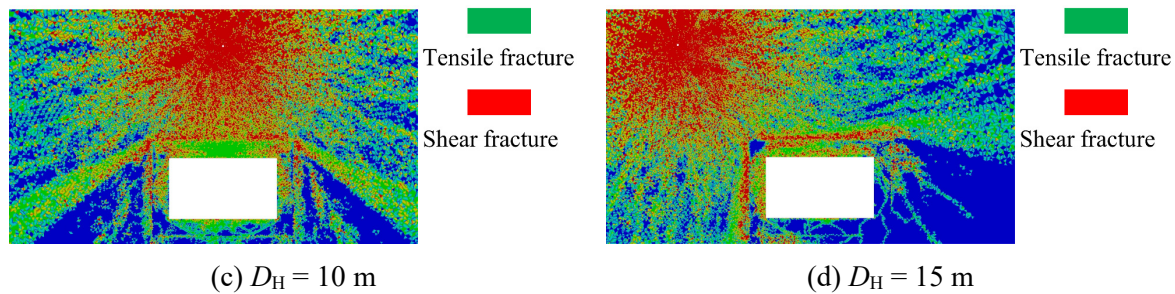

(a) $D_H = 0$ m

(b) $D_H = 5$ m

(c) $D_H = 10$ m   (d) $D_H = 15$ m
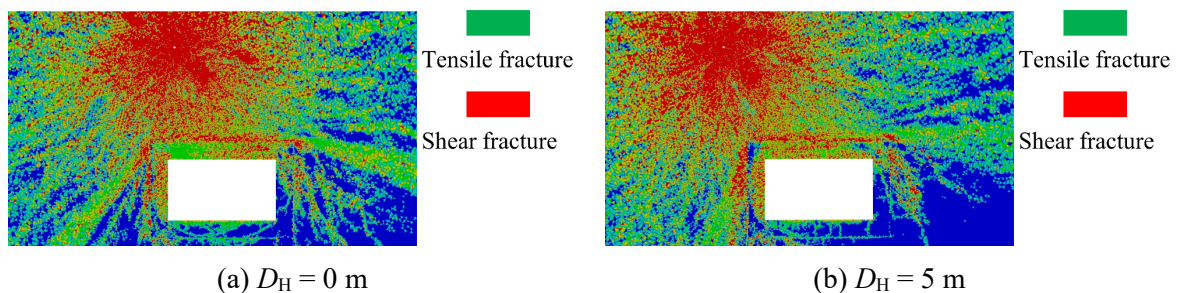
Figure 5. Crack nephograms of underground fortifications and rock mass

3. Conclusions

According to the continuum-discontinuum element method, the difference in mechanical responses of underground fortifications subjected to blast loading at different horizontal distances is studied.

(1) As the horizontal distance D_H increases from 0.0 m to 15.0 m, the maximum value of displacement of underground fortifications gradually decreases, changing from 3.35 m to 1.90 m, and the spatial distribution of displacement changes with the increase of horizontal distance D_H. In addition, the volume V_C and the volume V_F of rock mass gradually decrease with the increase of D_H.

(2) The growth curve of crack ratio α in different cases does not change significantly, and the crack ratio α at the same moment gradually decreases with the increase of D_H. The underground fortifications and rock mass not only undergo shear fracture, but also undergo tensile fracture, and the distribution of fracture types of underground fortifications changes significantly with the increase of D_H.

References

[1] Fan S B, Wang S L, Jia B, Wang W P and Cheng X J. (2019) Research on the correlation between burst depth and damage of typical underground works. Protective Engineering, 41: 8-11.

[2] Zhang L, Wu H, Zhao Q, Wang X, Ren X J, Wang J M and Kong D F. (2021) Calculation method of damage effects of underground engineering objectives on data mining technology. Explosion and Shock Waves, 41: 4-13.

[3] Meng Q F, Wu C Q, Li J, Wu P T, Xu S C and Wang Z Q. (2021) A study of pressure characteristics of methane explosion in a 20 m buried tunnel and influence on structural behavior of concrete elements. Engineering Failure Analysis, 122: 105273.

[4] Jiang N and Zhou C B. (2011) Mechanical responses characteristics of existing railway tunnel structure subjected to blasting vibration. China Railway Science, 32: 63-68.

[5] Ma W. (2008) Experimental investigations on effects of blast vibration and behaviors of impacting failure of underground pipeline structures. Journal of PLA University of Science and Technology, 9: 39-46.

[6] Fan P X, Wang M Y, Feng S F, Li J and Wang D R. (2013) Analysis of mechanical responses of deep-buried circular tunnel to explosion seismic wave. Chinese Journal of Rock Mechanics and Engineering, 32: 671-680.

[7] Zhao D B, Chu C and Su D. (2020) Mechanical responses of tunnel lining structure under internal blasts. China Civil Engineering Journal, 53: 265-271.

[8] Ma L J, Liu X Y, Ma Q L, and Sun B. (2011) On mechanical responses of large-span revetment structures subjected to blast loads in rock medium. Journal of China Coal Society, 36: 416-420.

[9] Kong D Q, Sun H X, Kang T and Ma T. (2014) The influence of rock characteristics on dynamic interaction between adjoining rock and structure subjected to blast loading. Journal of Air Force Engineering University (Natural Science Edition), 15: 77-81.

[10] Rashiddel A, Kharghani M, Dias D and Hajihassani M. (2020) Numerical study of the segmental tunnel lining behavior under a surface explosion-Impact of the longitudinal joints shape. Computers and Geotechnics, 128: 103822.

[11]Zhu J B, Li Y S, Wu S Y, Zhang R and Ren L. (2018) Decoupled explosion in an underground opening and mechanical responses of surrounding rock masses and structures and induced ground motions: A FEM-DEM numerical study. Tunnelling and Underground Space Technology, 82: 442-454.